

FRACTURE OF RUBBER-TOUGHENED POLY(METHYL METHACRYLATE): MEASUREMENT AND STUDY OF COHESIVE ZONE PARAMETERS

L. Andena and M. Rink

Dipartimento di Chimica, Materiali e Ingegneria Chimica, Politecnico di Milano, Italy

ABSTRACT

The fracture properties of a Rubber-Toughened Poly(Methyl Methacrylate) (RT-PMMA) have been investigated using a cohesive zone approach. The Circumferentially Notched Tensile (CNT) test configuration was used to directly measure traction-separation laws (TSL). Tests were performed at three different temperatures, with the same level of constraint. The cohesive zone parameters dependency on temperature was studied; the initial slope of the curve, the maximum cohesive stress, the critical separation and the overall fracture energy (i.e. the area under the TSL) were considered. They were compared with relevant material properties which were available in the literatures: modulus, yield stress and Schapery's fracture energy 2Γ . It was found that for the same level of constraint the initial slope vs. modulus, maximum cohesive stress vs. yield stress and fracture energy vs. 2Γ ratios are independent of temperature. Fracture energy values are much higher than 2Γ , while the maximum cohesive stress is 75% of the yield stress. The critical separation was found to increase with increasing temperature.

A cohesive law was derived from SENB tests at room temperature using an iterative inverse method based on a finite element model. This law has been compared with the CNT traction law obtained at the same temperature. The cohesive parameters differ, suggesting that cohesive laws are not intrinsic but depend on the stress state and thus on testing configuration. The fracture energy of the SENB cohesive law is very close to 2Γ measurements performed on the same testing configuration.

The two traction laws were used in a finite element model in order to simulate the load vs. displacement curve of a SENB test. Neither has proven able to give fully satisfactory results.

1 INTRODUCTION

Polymers viscoelastic nature is responsible for the intrinsic time-dependence of their mechanical properties. Their small deformation behaviour can well be described by the theory of linear viscoelasticity. However, when it comes to higher deformations, nonlinearities arise, followed by yielding and fracture. All these phenomena are time-dependent in the case of polymers.

Linear Elastic Fracture Mechanics (LEFM) has proven to be adequate in order to predict fracture for materials which exhibit a linear elastic behaviour. Fracture properties may be defined in term of a critical stress intensity factor K_C or a critical energy release rate G_C . These parameters are related and they can be easily measured performing standard Fracture Mechanics (FM) tests on notched specimens. However, polymers are intrinsically viscoelastic and these criteria may be inadequate.

Schapery's viscoelastic fracture theory [1-3] describes crack initiation and propagation in a viscoelastic medium. Schapery relies on the process zone concept originally introduced by Barenblatt: this is a small zone ahead of the crack tip where material degradation and separation occur. No assumptions are made regarding the behaviour of the material inside the process zone and the stress concentration at the crack tip is described through the stress intensity factor, K . The

work done by the viscoelastic medium over the process zone is the driving force for the fracture process: Schapery calculated it in term of the material viscoelastic functions and of the loading history. A crack initiates when this work equals a critical value for the material, defined as the fracture energy 2Γ . This energy can be determined from standard FM tests, provided that the initiation time is recorded and viscoelastic functions for the material (i.e. compliance or modulus) are known from independent experiments.

A more recent approach to analyze fracture is to determine (experimentally or via identification procedures) “traction-separation laws” (TSL) which describe the behaviour of the material in the process zone ahead of the crack. Such a cohesive law may be used to predict fracture with numerical modelling (for example with the finite element method). Direct in-situ characterization of the process zone has been performed by Pandya and Williams [4-6] who described the fracture behaviour of different grades of polyethylene by using TSLs determined from tensile tests performed on circumferentially notched tensile (CNT) specimens. For this material the constraint conditions promoted by this geometry give rise to a macroscopic process zone; the traction law may be identified measuring the overall load and the opening displacement of the notch.

Mariani et al. [7-8] studied the deformation and fracture behaviour of a rubber toughened poly(methyl methacrylate) (RT-PMMA). They applied Schapery’s theory to FM test results on single edge notched bending (SENB) and tension (SENT) specimens. They obtained fracture energy values as a function of time and temperature. In this work the same material was investigated performing tensile tests on CNT specimens and comparing results with Mariani et al. [7-8]. A method was also applied to identify a cohesive law from SENB tests and compare it with TSLs obtained from CNT specimens. This procedure involves the use of an iterative inverse method based on finite element (FE) simulations which was developed by Bianchi et al. [9]. Finally, the SENB tests have been simulated using a cohesive zone FE model using both the SENB and the CNT traction-separation laws.

2 EXPERIMENTAL

The material studied was a RT-PMMA with 22 wt% of acrylic rubber, supplied in the form of extruded sheets with nominal thickness $B = 7.5$ and 9.5 mm. The glassy matrix has weight and number average molecular weights of 134000 and 68000, respectively. The glass transition temperature of the matrix is 105°C , while that of the rubbery phase is -30°C . Two test configurations were considered, tensile full notch and single edge notched bending.

CNT specimens were obtained by cutting rectangular bars with dimensions of $7.5 \times 7.5 \times 95$ mm and $9.5 \times 9.5 \times 95$ mm. Different notch depths were introduced in the specimens, with ligament to bulk area (LBA) ratios ranging between 0.037 and 0.078. A lathe with a single point cutting tool was used to produce the 30° angled notches.

The SENB specimens had width W twice the thickness B and the span S was four times W . Notching was performed in two stages. In the first stage a notch was made with a $15 \mu\text{m}$ radius blade moving alternatively into the specimen. In the second stage, the same blade was pushed into the previously prepared notch after cooling the material to -40°C so as to propagate a short brittle crack. The blade works as a wedge and causes the formation of a natural crack ahead of the machined notch. The highly stressed zone that developed ahead of the notch tip during the machining operation was removed by annealing the specimens at 90°C for 5 h and then cooling them to 23°C at a rate of $1^{\circ}\text{C}/\text{min}$. A notch depth a_0 was produced, corresponding to an a_0/W ratio of about 0.55. No side grooves were made, in order to allow measurement of the crack tip opening displacement (CTOD).

CNT tests were performed at 23, 50 and 70°C with a constant crosshead speed of 0.05 mm/min. SENB specimens were tested at 23°C with a constant crosshead speed of 0.2 mm/min. All tests were conducted on a Instron 1185 dynamometer using a 10 kN load cell to measure the load P.

Separation and CTOD for CNT and SENB tests were measured using a Trio VE5000 video extensometer. The VE5000 can measure displacements with a spatial resolution of 1 μm .

3 RESULTS AND DISCUSSION

Traction-separation laws obtained from CNT specimens are shown in Figure 1. The cohesive stress was determined by dividing the load to the initial ligament section while the displacement was directly measured with the video extensometer. The effect of LBA ratio on TSL of RT-PMMA was found to be negligible in the range considered (0.037-0.078).

At 23°C crack propagation was stable only up to a separation of less than 0.15 mm and then the samples failed in a brittle way. As a consequence it was not possible to obtain the whole traction law from CNT tests at this temperature. At 50°C failure occurred at a later stage, when the softening was nearly completed; at 70°C the whole curve could be observed.

Several cohesive parameters were considered and their dependency on temperature was studied in comparison with modulus, yield stress and 2Γ data obtained by Mariani et al. (see Table 1).

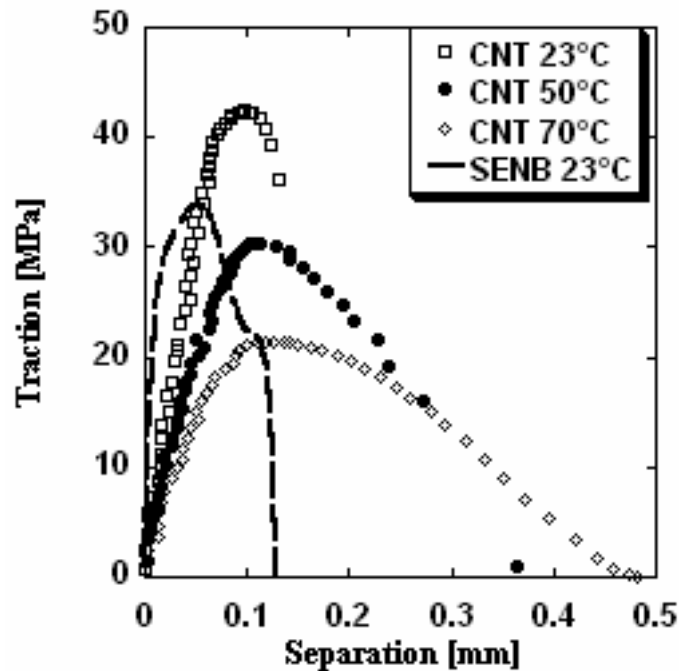


Figure 1: Traction-separation laws for CNT and SENB specimens

Table 1: Summary of results

<i>Test</i>	<i>Init slope</i> [N/mm ³]	<i>Modulus to</i> <i>init slope</i> <i>ratio</i> [mm]	<i>Max</i> <i>Stress</i> [MPa]	<i>Max stress</i> <i>to Yield</i> <i>stress ratio</i>	<i>Max</i> <i>separation</i> [mm]	<i>Fracture</i> <i>Energy</i> [kJ/m ²]	<i>Fracture</i> <i>Energy to</i> <i>2Γ ratio</i>
SENB 23°C	3500	0.6	34	0.61	0.13	3.3	1.1
CNT 23°C	640	3.3	42	0.75	-	-	-
CNT 50°C	350	4.0	30	0.75	0.37	6.9	2.3
CNT 70°C	300	3.3	21	0.75	0.47	6.2	2.4

It can be seen that the initial slope of the traction-separation laws obtained decreases with temperature. This slope was compared with modulus at the relevant temperature and time and their ratio gives a characteristic length. The initial part of traction-separation laws represents elastic deformation of the small volume of material which will eventually originate the process zone. Since the characteristic length is approximately constant, the volume of material involved in the fracture process at different temperatures is about the same.

The maximum cohesive stress is found to be decreasing with temperature and it is equal to 75% of the corresponding yield stress. Therefore, for a given testing configuration and constraint level, the yielding stress controls the dependency of the cohesive strength on temperature. For metals maximum cohesive stress is usually 2-2.5 times the yield stress but for polymers this is not the case, as shown by Pandya and Williams [4,5].

The critical separation at 70°C is greater than at 50°C. It could not be determined at 23°C but the general shape of the curves suggests that this quantity increases with increasing temperature.

The area under the traction-separation curve is the surface fracture energy of the material. Values obtained from these curves at 50 and 70°C are much greater than 2Γ values determined by Mariani et al. on SENB specimens. However, the ratio between fracture energy and 2Γ appears to be independent of temperature.

A cohesive law was derived from SENB tests at 23°C using an iterative procedure, based on a finite element model originally developed by Bianchi et al. [9]. The bulk material is considered linear elastic while fracture is described by interface elements with a linear stepwise cohesive law. The procedure inputs are global load and measured CTOD. A small load is applied in the FE model and the initial slope of the cohesive law is adjusted to match the CTOD with experiment. The first step of the cohesive law is then known, up to a certain value of opening displacement. Load is subsequently increased by a small amount: the crack tip node is thus forced to a higher value of opening displacement while the other nodes along the crack path stay on the first step. The slope of the second step is again adjusted matching the CTOD with the experimental measurement for the new value of applied load. Once the second step is determined load can be increased and the whole cohesive law can be obtained by successive iterations (see Figure 1). The procedure ends at crack initiation, when the crack tip node reaches the critical opening displacement and the traction becomes zero. This method can be used even on materials that exhibit a brittle behaviour, for which traction laws cannot be directly determined.

The initial slope of SENB TSL curve was more than five times than the slope of the 23°C CNT traction law. This indicates that the volume of material originating the process zone is smaller for SENB configuration. The maximum cohesive stress and the critical separation for SENB are lower than those of the CNT traction law. As a consequence, the fracture energy is much lower: its value is only 10% higher than 2Γ measurements performed by Mariani et al. in the same configuration. This gap could be due to the presence of side grooves in Mariani's specimens.

The same FE model adopted for the identification procedure has been used with the SENB cohesive law to simulate the relevant experimental load vs. displacement curve. FE simulations were performed using an arclength method to ensure convergence during the softening stage. It must be noted that the SENB law has been identified from load vs. CTOD data up to initiation. The outcome of simulation is shown in Figure 2. There is perfect agreement with the experimental load vs. displacement curve only up to a load of about 190 N corresponding to predicted crack initiation. After that, the model predicts an abrupt decrease in load while the experiment shows a further increase up to 196 N, followed by a smoother decrease. The following softening branch almost coincides with the predicted one. It is clear that some energy contribution is missing, probably due to viscoelasticity or plasticity in the bulk material (as the fracture energy is already higher than 2Γ). Another possible reason could be the variation of constraint consequent to crack propagation. This hypothesis will be investigated in the future work.

A simulation has been performed with the same FE model using the CNT traction law in place of the SENB cohesive law. The traction-separation curves has been extrapolated to zero stress using a 5th degree polynomial fitting. Extrapolated critical CTOD and fracture energy were 0.16 mm and 4.7 kJ/m² respectively, with a fracture energy to 2Γ ratio of 1.58. This last value seems quite low in comparison with CNT laws at 50 and 70°C but it must be noted that most of the softening branch in the 23°C curve is missing. The shape of the other two curves suggests that its slope might be lower than that obtained by extrapolation. Figure 2 shows the predicted load vs. displacement curve for the SENB test. The agreement in the first part of the curve is not as good as using the SENB cohesive law. The peak load is overestimated by 15% and this is a consequence of the high value of fracture energy associated with the CNT traction law. The prediction of the softening branch is accurate; however, if the whole traction-separation law could be determined, it is likely that the simulation would yield a softer response.

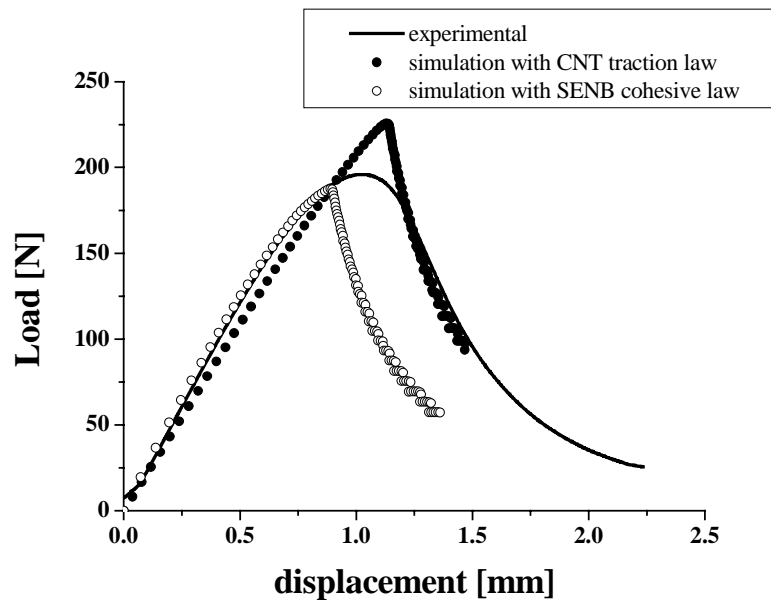


Figure 2: Prediction of SENB load vs. displacement curve using cohesive zone modelling

Further work is needed to achieve a better understanding of the influence of the stress state on traction laws. Moreover, the simple FE cohesive model used must be improved, since it has proven unable to yield accurate predictions of SENB tests.

ACKNOWLEDGMENTS. The authors would like to thank Prof. J.G. Williams of Imperial College (London, UK) for his valuable comments.

REFERENCES

1. R.A. Schapery, **A theory of crack initiation and growth in viscoelastic media I. Theoretical development**, *International Journal of Fracture*, 11, 141-159 (1975)
2. R.A. Schapery, **A theory of crack initiation and growth in viscoelastic media II. Approximate methods of analysis**, *International Journal of Fracture*, 11, 369-388 (1975)
3. R.A. Schapery, **A theory of crack initiation and growth in viscoelastic media III. Analysis of continuous growth**, *International Journal of Fracture*, 11, 549-562 (1975)
4. K.C. Pandya, J.G. Williams, **Measurement of Cohesive Zone Parameters in Tough Polyethylene**, *Polymer Engineering and Science*, 40, 8, 1765-1776 (2000)
5. K.C. Pandya, J.G. Williams, **Cohesive zone modelling of crack growth in polymers Part 1 – Experimental measurement of cohesive law**, *Plastics, Rubber and Composites*, 29, 9, 439-446 (2000)
6. K.C. Pandya, A. Ivankovic, J.G. Williams, **Cohesive zone modelling of crack growth in polymers Part 2 – Numerical simulation of crack growth**, *Plastics, Rubber and Composites*, 29, 9, 447-452 (2000)
7. P. Mariani, R. Frassine, M. Rink, A. Pavan, **Viscoelasticity of Rubber-Toughened Poly(Methyl Methacrylate). Part I: Deformational Behavior**, *Polymer Engineering and Science*, 36, 22, 2750-2757 (1996)
8. P. Mariani, R. Frassine, M. Rink, A. Pavan, **Viscoelasticity of Rubber-Toughened Poly(Methyl Methacrylate). Part II: Fracture Behavior**, *Polymer Engineering and Science*, 36, 22, 2758-2764 (1996)
9. S. Bianchi, A. Corigliano, R. Frassine, M. Rink, **Modelling of Interlaminar Fracture Processes in Composites using Interface Elements**, submitted to *Composites Science and Technology* (2003)